Angewandte Chemie
Eine Zeitschrift der Gesellschaft Deutscher Chemiker

Supporting Information

Anisotropic Conductivity at the Single-Molecule Scale

*Sepideh Afsari, Parisa Yasini, Haowei Peng, John P. Perdew, and Eric Borguet**

anie_201903898_sm_miscellaneous_information.pdf

SUPPORTING INFORMATION

Abstract: In most junctions built by wiring a single molecule between two electrodes, the electrons flow along only one axis: between the two anchoring groups. However, molecules can be anisotropic and an orientation-dependent conductance is expected. Here, we fabricate single molecule junctions using the electrode potential to control the molecular orientation and access individual elements of the conductivity tensor. We measure the conductance in two directions; along the molecular plane as the benzene ring bridges two electrodes using anchoring groups (upright); and orthogonal to the molecular plane with the molecule lying flat on the substrate (planar). The perpendicular (planar) conductance is ~400 x higher than along the molecular plane (upright). This offers a new method for designing a reversible single molecule electromechanical switch that at room-temperature controllably employs the electrode potential to orient the molecule in the junction between “ON” and “OFF” conductance states.

DOI: 10.1002/anie.2016XXXXX

SUPPORTING INFORMATION

Table of Contents

Experimental Procedures

1. Materials and methods

a. Chemicals and Solutions

Trimesic acid, TMA (1,3,5-benzenetricarboxylic acid), (95%, Sigma-Aldrich)
Pyromellitic acid, PMA (1,2,4,5-benzenetetracarboxylic acid), (96% Sigma-Aldrich)
1 mM TMA in 0.05 M H_2SO_4
1 mM PMA in 0.05 M H_2SO_4
For preparing self-assembled monolayers in acidic solutions under electrode potential control, molecular solutions in 0.05 M H_2SO_4 (99.999%, Sigma Aldrich) were used as the electrolyte.

b. STM cell set up and sample preparation: An Au(111) single crystal disk, on which wide (~100 nm) terraces could be easily found, was used as the substrate. Before all experiments, the substrate, the Teflon cell and the O-ring (Viton) were cleaned by immersion in hot piranha solution (1:3 H_2O_2 (J. T. Baker, CMOS)/ H_2SO_4 (96%, J. T. Baker, CMOS) for 1h. (Caution! The piranha solution is a very strong oxidizing reagent and can be dangerous. Protective equipment including gloves and glasses should be used at all times). They were then rinsed and placed, for a few minutes, in boiling ultrapure deionized (DI) water obtained from a Thermoscientific Barnstead Easypure II purification system equipped with a UV lamp (water resistivity >18 MΩ.cm). A hydrogen flame was used to anneal the crystal, followed by quenching in hydrogen-saturated ultrapure DI water. The Au disk, Teflon cell and O-ring were dried under a stream of Ar. Then the cell was quickly set up, solvent was added to cover the electrode and the cell was installed in the microscope.

c. Electrochemical Scanning Tunneling Microscopy (EC-STM) Imaging: STM images were obtained with a PicoScan STM system (Molecular Imaging). The PicoStat bipotentiostat (Molecular Imaging) was used to control the surface and tip potential independently. Platinum wires were used as the quasi-reference electrode and the counter electrode. STM tips were prepared by electrochemically etching 0.25 mm diameter tungsten wires in 2 M NaOH solution using a platinum ring electrode. Tips, coated with polyethylene, yielded less than 10 pA Faradic current. All the STM images were obtained under constant current mode. Additional details of the STM experiment can be found in the caption of each image reported.

d. Electrochemical Scanning Tunneling Microscopy Break Junction (EC-STM-BJ): The Electrochemical STM break junction (EC-STM-BJ) experiments were carried out with a Keysight Picoscan (Molecular Imaging) microscope under electrode potential control. 1 μA/V and 10 nA/V pre-amplifiers were used for all SMC measurements. STM software drove the tip to approach the gold surface in the STM cell while the surface and the tip potentials were controlled using the PicoStat bipotentiostat. In STM break junction (STM-BJ) experiments, the STM tip is repeatedly brought into and out of contact with another electrode in the presence of molecules while current-distance traces are recorded. The displacement of the two electrodes (the STM tip and the substrate) without molecules bridging between them gives rise to quasi

exponentially decaying traces. When a molecular junction forms, the current remains approximately constant even as the electrode-electrode distance increases so that a current plateau or step appears in the traces. The current drops exponentially with distance when the junction breaks. The histogram generated from the measured current-distance traces contains peaks that can be ascribed to charge transport through single molecules. Thus, the conductance of single molecules can be determined. For individual current-distance traces, the tip was driven into contact with the substrate to form a junction at a sweep rate of 16-26 nm/s. The tip was then retracted to break the contact. The process of the forming and breaking of junctions was repeated many times and a large number of current-distance traces were recorded for statistical analysis.

e. STM-BJ data analysis: To generate each histogram, more than 2000 individual current-distance traces were collected and analyzed without selection. Current-distance traces were collected only when the individual curves showed current saturation reflecting tip-surface contact, followed by sharp decay of current after pulling the tip away from the surface. As soon as the curves no longer showed current saturation at the tip-surface contact, we stopped recording data, repositioned the tip and resumed measurements. Data collection restarted when current saturation could be achieved for the tip-surface contact.

f. Fabricating single gold atom junction and quantum conductance (Go) measurements: For creating single gold atom junction, the sharp gold tip is repeatedly driven into full contact and out of contact with gold crystal substrate while current-distance traces are recorded (Figure S1 A). The withdrawal of the tip gives rise to quasi exponentially decaying traces. When a connective neck with one or multiple gold atoms bridging between the tip and the gold substrate is formed, the current remains approximately constant and give rise to a current plateau or step in the traces (Figure S1 B). The current drops exponentially with distance when the junction breaks. The histogram generated from the measured current-distance traces contains peaks that can be ascribed to charge transport through the junction and one-atom gold conductance can be extracted from the position of the peaks in the histogram (Figure S1 C).

g. STM-BJ Control experiments on Au(111) surface at high conductance region: All experiments were carried out with a Keysight Picoscan (Molecular Imaging) microscope and 1 μA/V pre-amplifier was used for the SMC measurements.

I. STM-BJ of TMA in 0.05M H_2SO_4 on Au(111) without potential control: Experiments were carried out with no electrode potential control in the presence of 1 mM TMA in 0.05 M H_2SO_4 solution while the bias voltage (E_{bias}) of -0.10 V applied between the Au(1111) electrode and the tip. The histogram is constituted of 10232 current-distance traces without any data selection.

II. STM-BJ of 0.05M H_2SO_4 without TMA on negatively charged Au(111): Experiments were carried out under electrode potential control using the PicoStat bipotentiostat in 0.05 M H_2SO_4 solution on a negatively charged Au(111) substrate ($E_{surface}$ = -0.10 V_{SCE}) and the bias voltage (E_{bias}) of -0.10 V applied between the Au(1111) electrode and the tip. The histogram is constituted of 2634 current-distance traces without any data selection.

III. STM-BJ of Au(111) in air: Experiments were carried out with no electrode potential control. Current-distance traces were collected at air (in the absence of any electrolyte solution) with the bias voltage (E_{bias}) of -0.10 V applied between the Au(1111) electrode and the tip. The histogram is generated without any data selection of 2216 current distance traces.

Figure S1. Single gold atom junctions formation and conductance measurements using STM-BJ. A, Schematic for formation of a single gold atom junction using STM-BJ. **B,** Example of individual current-distance traces indicating current plateaus. **C,** The conductance histogram of all STM-BJ measurements on the Au(111) surface carried out at E_{bias}= -0.050 V without any data selection of more than 2000 individual current-distance traces.

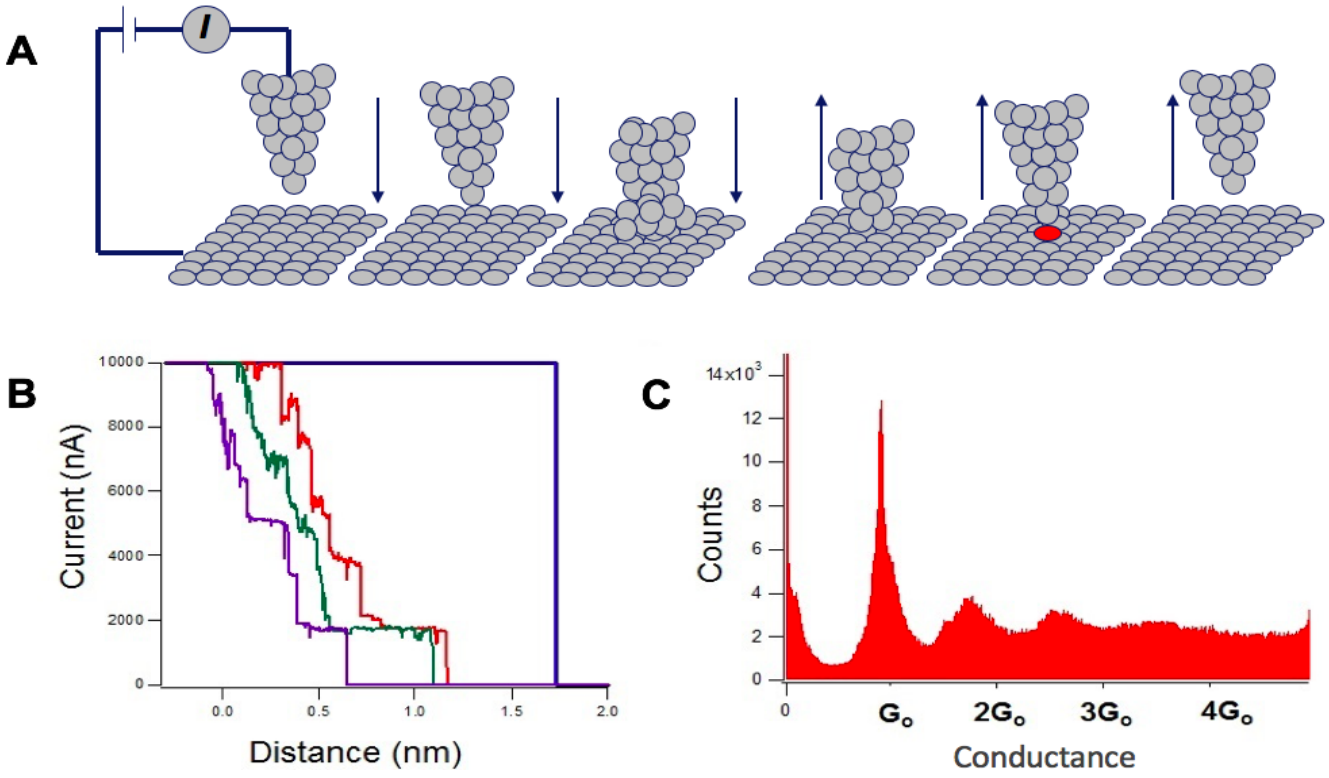
A
I
B
Current (nA)
10000
8000
6000
4000
2000
0
0.0
0.5
1.0
1.5
2.0
Distance (nm)
C
14x10^3
12
10
8
6
4
2
0
Counts
0
G0
2G0
3G0
4G0
Conductance

SUPPORTING INFORMATION

Results and Discussion

2. Analysis of EC-STM images of ordered structure of TMA on charged Au(111) surface

Cross section analysis of TMA in STM images indicates that the distance between the neighboring molecules in the long range ordered structures formed at negative and positive potentials (Figure S2 A a S2 C) is different. The distance between maxima, tentatively assigned to neighboring molecules adsorbed on the negatively charged Au(111) substrate (Figure S2 A), measured from the cross section of the ordered structure (blue line in Figure S2 A), is about 9 Å (Figure S2 B). This value is consistent with the characteristic end to end length of TMA reported in the literature suggesting that TMA molecules orient with the benzene ring parallel to the Au(111) surface on the negatively charged Au(111) substrate.

STM images of the positively charged Au(111) substrate (Figure S2 C) are characterized by identically aligned bright dots separated by about 3.5 Å (Figure S2 D) measured from the cross section of the ordered structure (blue line in Figure S2 C) consistent with the reported upright structure of TMA molecules. These paired bright dots are upright oriented dimer of TMA molecules with the parallel benzene rings.

Figure S2. Detailed STM images and cross section analysis of trimesic acid (TMA) on Au(111). A, 10×10 nm^2 STM images of TMA on a negatively charged ($E_{surface}$ = -0.10 V_{SCE}) Au(111) electrode. **B,** Cross section of the ordered structure in direction denoted by the blue line in image A. **C,** 10×10 nm^2 STM images of TMA on a positively charged ($E_{surface}$ = +0.75 V_{SCE}) Au(111) electrode. **D,** Cross section of the ordered structure in direction denoted by the blue line in image C. I_t= 0.08 nA, E_{tip} = 0.00 V_{SCE}.

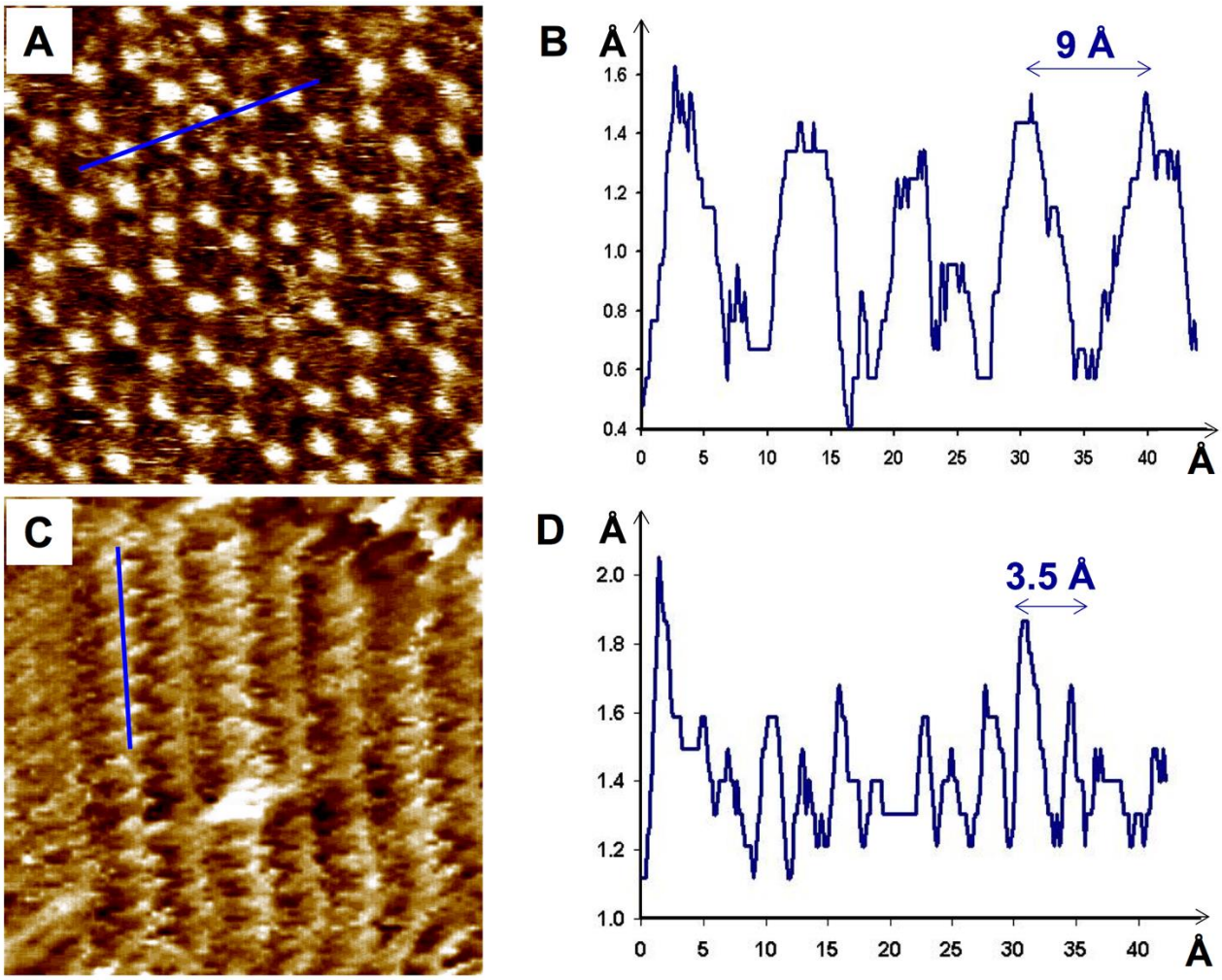

SUPPORTING INFORMATION

3. Conductance vs. bias in EC-STM-BJ measurements for trimesic acid (TMA) at high current regions

The current-bias relationship for the 0.15 Go peak was investigated by varying the bias voltage (E_{bias}) from -0.10 V to -0.05 V in SMC experiments while the electrode potential of the surface ($E_{surface}$) was kept at negative values and unvaried (-0.1 V_{SCE}). The current maxima in the histogram move to lower current regions proportionally to the E_{bias} (Figure S3) in accordance with Ohm's law (V= IR).

Figure S3. Current-bias relationship of trimesic acid (TMA) high conductance peak. A, All-data point EC-STM-BJ current histograms of TMA on negatively charged ($E_{surface}$ = -0.10 V_{SCE} and E_{bias} = -0.10 V) without any data selection of 9070 individual current-distance traces, red arrows indicating 0.15 G_o and G_o peaks. **B,** All-data point EC-STM-BJ current histograms of TMA on negatively charged ($E_{surface}$ = -0.10 V_{SCE} and E_{bias} = -0.050 V) without any data selection of 1608 individual current-distance traces, green arrows indicating 0.15 G_o, G_o and 2 G_o peaks.

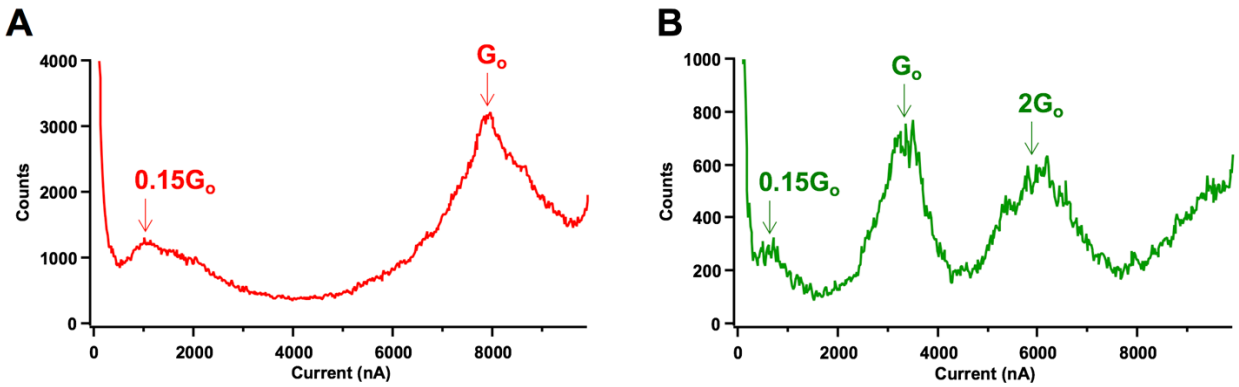

SUPPORTING INFORMATION

4. Conductance vs. bias in EC-STM-BJ measurements for trimesic acid (TMA) at low current regions

The current-bias relationship for two low conductance peaks at 0.0004 Go and 0.0009 Go was investigated by varying the bias voltage (E_{bias}) from -0.10 V to higher values at -0.30 V in SMC experiments while the electrode potential of the surface ($E_{surface}$) was kept at positive values and unvaried (+0.75 V_{SCE}). The current maximum in the histogram moves toward higher currents proportionally to the E_{bias} (Figure S4) in accordance with Ohm's law (V= IR).

Figure S4. Current-bias relationship of trimesic acid (TMA) low conductance peak. A, All-data point EC-STM-BJ current histograms of TMA on positively charged ($E_{surface}$ = +0.75 V_{SCE} and E_{bias} = -0.10 V) without any data selection of 2974 individual current-distance traces, blue arrows indicating two low conductance peaks at 0.0004 G_o and 0.0009 G_o. **B,** All-data point EC-STM-BJ current histograms of TMA on positively charged ($E_{surface}$ = +0.75 V_{SCE} and E_{bias} = -0.30 V) without any data selection of 2027 individual current-distance traces, green arrows indicating two low conductance peaks at 0.0004 G_o and 0.0009 G_o moved toward higher currents.

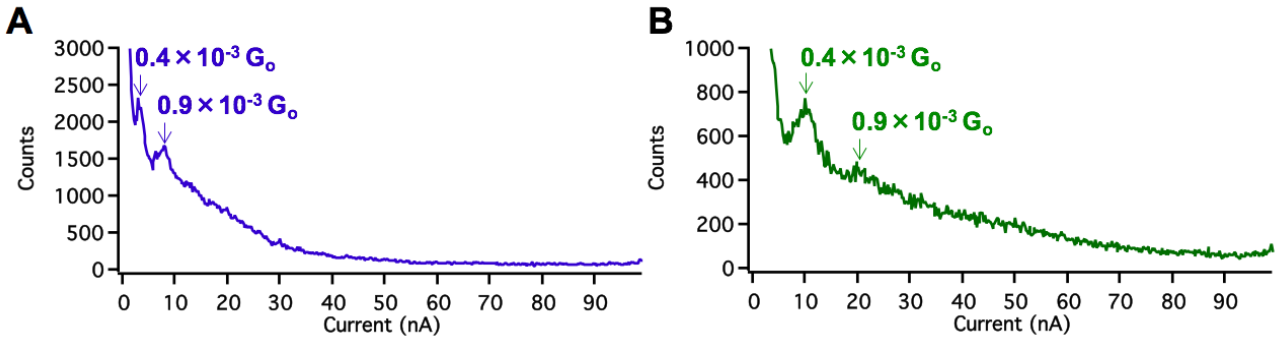

5. Conductance measurements of pyromellitic acid (PMA) on a charged Au(111) surface at low current regions

Figure S5. EC-STM-BJ of pyromellitic acid (PMA) on a charged Au(111) at low current regions. A, All-data point EC-STM-BJ current histograms of PMA collected on negatively charged ($E_{surface}$ = -0.10 V_{SCE} and E_{bias}= -0.10 V) without any data selection of 2008 individual current-distance traces. **B,** All-data point EC-STM-BJ current histograms of PMA collected on positively charged ($E_{surface}$ = +0.75 V_{SCE} and E_{bias}= -0.30 V) without any data selection of 1982 individual current-distance traces.

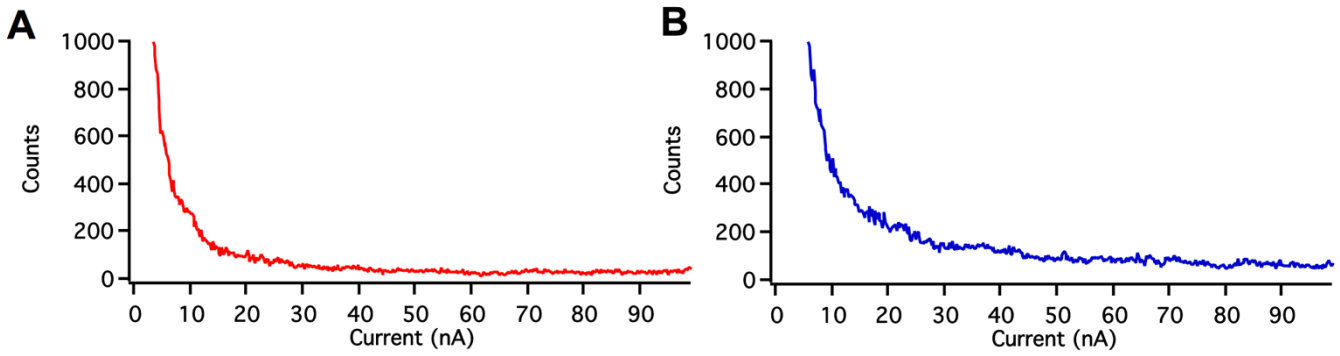

6. Computation details for the structure modelling

For the flat configuration, a 5-layer 4 ×4 × 1 supercell is used to model the Au(111) surface. We first determine the structure of the molecular junction as shown in the left panel for Figure S6, which, from the bottom to the top, contains the 5-layer Au(111) surface electrode, the molecule with the so-called hcp-A configuration, the 3-layer Au(111) tip, another 5-layer Au(111) surface, and a vacuum layer of about 15 Å. We change the distance between the top and bottom Au triple-layers by a step of 0.1 Å, and let the other atoms fully relax until the residual forces are smaller than 0.04 eV/Å. Then the resulting lowest energy structures with the vacuum layer removed are used for the following NEGF calculations (Middle panel in Figure S6 for the flat configuration). A similar procedure was applied to obtain the structure for the vertical configuration (Figure S6 Right panel), where the bottom hydrogen atom was removed and the Au-O bonds forms as the anchoring group as suggested by the experiments.

Figure S6. Schematic illustration for the structure modeling in this work. Left: the supercell for the flat configuration with which we vary the electrode-substrate distance *d* manually and relax the atoms between the two bottom and top triple-layers; Middle: the final lowest-energy (as function of *d*) supercell with the vacuum layer removed for following transport calculation, where semi-infinite electrodes will be attached to both ends; Right: similar to Middle but for the vertical configuration.

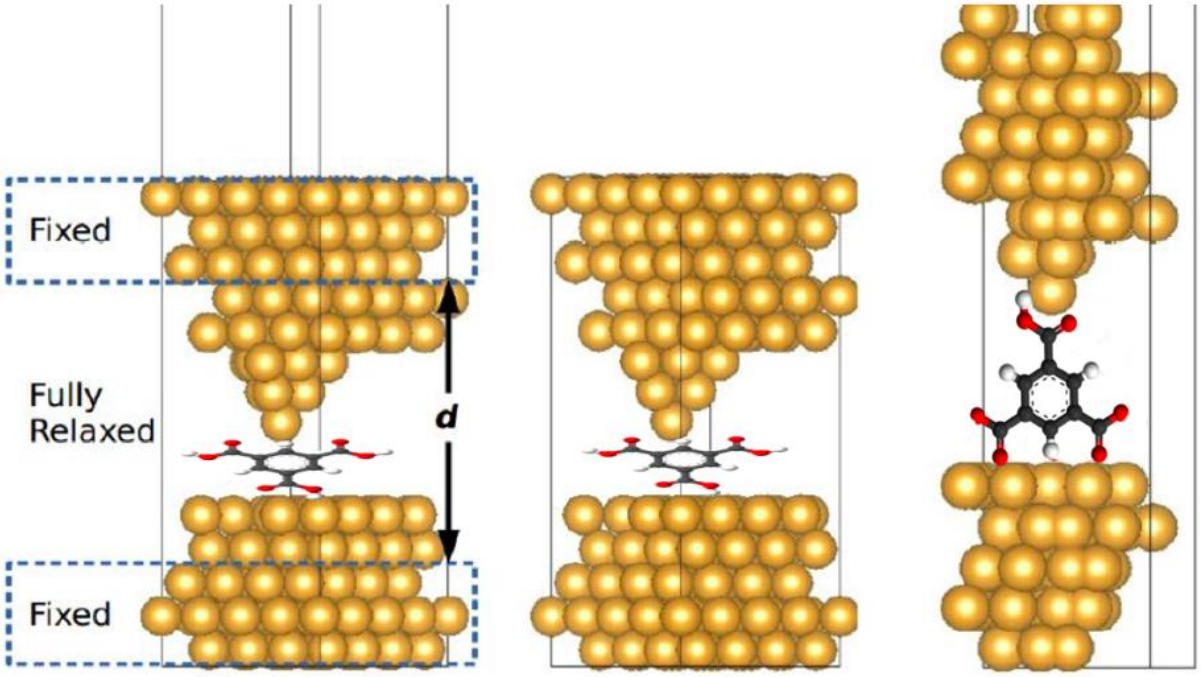

Author Contributions

S.A. and E.B. designed the experiments. S.A. designed sample preparation procedures. S.A. performed the STM imaging experiments. S.A. and P.Y. performed the STM-BJ experiments. H.P performed DFT calculation and modeling. S.A. and E.B. wrote the experimental part, H.P and J.P.P wrote the theory part and all authors commented on the manuscript.